Systematic design of unimolecular star copolymer micelles using molecular dynamics simulations†

Loan Huynh,[a] Chris Neale,[b] Régis Pomès[b] and Christine Allen*[a]

Received 29th January 2010, Accepted 30th June 2010
DOI: 10.1039/c001988g

Star copolymers (SCPs) have recently attracted considerable attention due to their unique applicability in a wide range of biomedical fields. With the intention of rationally designing a stable unimolecular SCP, atomistic molecular dynamics simulations of thirteen SCPs are conducted. The SCPs each have six identical arms of methoxypoly(ethylene glycol)-*b*-polycaprolactone ($MePEG_x$-*b*-PCL_y) and systematically vary in terms of total molecular weight and ratio of hydrophobic to hydrophilic block length. For all hydrated SCPs, the simulations predict a densely packed hydrophobic PCL core that excludes water and is phase separated from a highly mobile hydrophilic PEG corona. The radii of the hydrophobic PCL core and the PEG blocks are independent of each other and can be predicted over a broad molecular weight range. A linear relationship between the hydration and the molecular weight of the PEG blocks is observed with the average number of water molecules bound per PEG repeat unit within the range of that determined experimentally. As well, a quantitative relationship relates the water accessed surface area of the hydrophobic PCL core to the molecular weights of PCL and PEG moieties. We postulate that the propensity for aggregation of SCPs into multimolecular micelles is correlated with the partial hydration of the hydrophobic core of unimers. Our results suggest that SCPs with a hydrophobic PCL core ≤2 kDa per arm are fully protected from water when the hydrophilic PEG blocks approach 14.6 kDa per arm. We therefore predict that SCPs of this composition yield unimolecular micelles that are thermodynamically stable at low concentrations.

1 Introduction

Linear, amphiphilic diblock and triblock copolymers have emerged as the materials of choice for use in a wide range of biomedical applications, including fabrication or coating of biomedical devices, drug delivery, and tissue engineering.[1–4] The use of block copolymers in these technological platforms brings unparalleled diversity since they can be synthesized such that they self-organize or self-assemble, under specific conditions, to form superstructures with dimensions on the order of the nano- or micrometre.[5] Self-organization of these materials into ordered structures is reliant on the presence of specific intra- or intermolecular interactions. Understanding the relationship between the composition of these materials and the self-organized superstructures they form is necessary for their rational design and use in particular applications.

Recent advances in synthetic procedures have afforded controlled preparation of block copolymers having complex architectures, such as dendrimer-like, graft-block, or star-block copolymers (SCPs).[6–8] In aqueous media amphiphilic SCPs, with central hydrophobic blocks surrounded by terminal hydrophilic blocks, can be used for the solubilization or delivery of hydrophobic solutes.[9,10] The hydrophobic core-forming blocks serve as cargo space for the lipophilic solutes while the hydrophilic blocks form a shell that protects the core from the aqueous environment. SCPs can form unimolecular or multimolecular micelles depending on the copolymer composition and architecture.[9,11,12] Of particular interest, SCPs that form unimolecular micelles are not faced with issues relating to thermodynamic instability and may be prepared to be smaller in size with a more narrow size distribution than most multimolecular systems.[13,14] To date, numerous SCP systems have been put forth in an attempt to design unimolecular micelles. These SCPs include star amphiphilic block copolymers based on poly(ethylene glycol)-*b*-polycaprolactone (PEG-*b*-PCL) and PEG-*b*-poly(L-lactide).[9,11] In only a few cases, however, have the solution properties of these systems been studied thoroughly.[9,11,12] As such, there remains a limited understanding of the relationship between the composition and architecture of SCPs (such as the number of arms, the nature and length of hydrophobic/hydrophilic blocks and the total molecular weight), their self-organizing behavior, and the properties of the unimolecular or multimolecular micelles that they form. As well, few studies have examined the structure, the hydration state of the inner hydrophobic core and outer hydrophilic corona-forming blocks, and the composition of the core–corona interface in SCP systems. These parameters influence important properties of the micelles, such as thermodynamic and kinetic stability, degradation profile, and solute loading capacity.

[a]*Leslie Dan Faculty of Pharmacy and Department of Chemistry, University of Toronto, 144 College Street, Toronto, ON, M5S 3M2, Canada. E-mail: cj.allen@utoronto.ca; Fax: +1 416 978 8511; Tel: +1 416 946 8594*
[b]*Molecular Structure and Function, The Hospital for Sick Children, 555 University Avenue, Toronto, ON, M5G 1X8, Canada. E-mail: pomes@sickkids.ca; Fax: +1 416 813 5022*

† Electronic supplementary information (ESI) available: Trajectory MD simulation movie of $[MePEG_{113}$-*b*-$PCL_{18}]_6$ SCP showing the highly mobile hydrophilic PEG corona and the compact hydrophobic PCL core is included. Additional figures are provided for the density profiles, the distribution of the end-to-end distance, the hydration and the R_g for $[MePEG_x$-*b*-$PCL_y]_6$ SCPs. Theoretical model for calculating asphericity index and Flory model for predicting the structural properties of PEG are also included. See DOI: 10.1039/c001988g

Computational methods have recently been used to study the behaviour of SCPs in unimolecular and multimolecular states.[15–18] However, the solution behaviors of these copolymers and their intermolecular interactions have not previously been explored in atomistic detail. This is likely due to the fact that significant computational resources are required for these large systems. The aim of our current study is to gain fundamental insight into the properties of SCPs in aqueous solution and to rationally design a stable unimolecular star copolymer by conducting all-atom molecular dynamics (MD) simulation studies of these systems in explicit water. The atomistic resolution of the simulations enables explicit treatment of the physical basis of molecular self-aggregation, including the interactions that underlie the hydrophobic effect. As a first step towards the rational/structure-based design of unimolecular micelles, in the present study the solution properties of differently composed SCPs as unimers are evaluated by MD simulation. Atomistic simulations of thirteen SCPs in water were carried out for a total simulation time of 200 ns for each system. The present study yields insight into the equilibrium conformations of the SCPs as well as detailed information on the hydrophobic PCL and hydrophilic PEG blocks, and their interactions with water, during self-organization. In light of the potential benefits of monodisperse unimolecular micelles, our study is focused largely on predicting the parameters that are likely to influence the equilibrium governing copolymer aggregation and micelle disassembly, indirectly probing the mechanism of aggregation. Dynamic and static light scattering revealed that six-armed $[MePEG_{113}$-b-$PCL_{18}]_6$ SCPs aggregate, forming multimolecular micelles in water (F. Li and C. Allen, unpublished results). The molecular basis of this unimeric instability is, however, difficult to assess experimentally due to the low concentrations required to obtain the unimeric state. In contrast, computer simulations permit the study of unimeric states in isolation. Here, we take advantage of this capability to examine the relationship between SCP composition and solvation, and to quantify the exposed hydrophobic surface area of the core. PEG coronas that completely protect the hydrophobic core from solvent during unimeric simulation are likely to displace the equilibrium governing aggregation toward the unimeric state.

Table 1 Composition of the $[MePEG_x$-b-$PCL_y]_6$ star copolymer systems used in the molecular dynamics simulations[a]

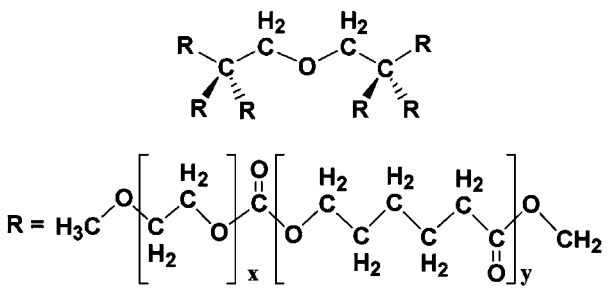

x–y	x : y ratio	Volume/ nm^3	Number of water molecules	M_{wPCL} per arm	M_{wPEG} per arm
6–1	6.0	164	5194	114	295
12–2	6.0	209	6566	228	560
19–2	9.5	349	11 053	228	868
19–3	6.3	333	10 482	342	868
27–2	13.5	504	16 021	228	1221
27–3	9.0	526	16 634	342	1221
27–4	6.8	476	15 023	456	1221
38–3	12.7	512	17 412	342	1705
38–4	9.5	504	15 778	456	1705
38–6	6.3	493	15 335	684	1705
38–9	4.2	557	17 365	1026	1705
113–18	6.3	3389	108 338	2052	5010
118–6	19.7	2797	89 429	684	5230

[a] x and y are the number of repeat units in the PEG and PCL blocks, respectively, of each arm in the $[MePEG_x$-b-$PCL_y]_6$ star copolymers.

2 Methodology

2.1 Simulated systems

The series of SCPs under investigation have six identical arms radiating from a small central core. The arms are composed of methoxyPEG (MePEG) and PCL (*i.e.* $[MePEG_x$-b-$PCL_y]_6$, Table 1). The thirteen systems simulated contain a single hydrated $[MePEG_x$-b-$PCL_y]_6$ SCP and vary systematically in terms of the degree of polymerization of the PEG, N_{PEG}, and PCL, N_{PCL}, in each arm (*i.e.* number of repeat units, x and y, respectively) as well as in terms of total M_w of the SCP and

Table 2 Parameters for the $CH_2OCOOCH_2$ fragment

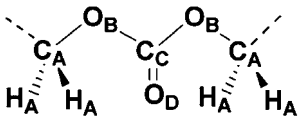

Atom types	Mass/g mol^{-1}	Charge/e	σ/nm	ε/kJ mol^{-1}
O_D	15.99940	−0.505	0.296000	0.878640
O_B	15.99940	−0.460	0.300000	0.711280
C_C	12.01100	0.799	0.375000	0.439320
C_A	12.01100	0.253	0.350000	0.276144
H_A	1.00800	0.003	0.242000	0.062760

Bond types	Bond length/nm	Bond stretching force constant/kJ mol^{-1} nm^{-2}
O_D C_C	0.12169	381 999.0
C_C O_B	0.13279	220 497.0
O_B C_A	0.14487	141 001.0
H_A C_A	0.10900	284 512.0

Angle types[a]	Angle/rad	Angle bending force constant/kJ mol^{-1} rad^{-2}
O_B C_C O_B	110.4	429.2784
O_D C_C O_B	124.8	430.5336
C_C O_B C_A	119.2	348.1088
O_B C_A H_A	109.5	292.8800
H_A C_A H_A	107.8	276.1440

Dihedral angle[b]	C_1/kJ mol^{-1}	C_2/kJ mol^{-1}	C_3/kJ mol^{-1}	C_4/kJ mol^{-1}
C_A O_B C_C O_D	21.43881	0	21.43881	0
C_A O_B C_C O_B	16.15810	1.683820	−14.73370	−3.10824
H_A C_A O_B C_C	0.41421	1.242650	0	−1.65686

[a] The H_A C_A H_A angle type was obtained from the standard OPLS-AA of alkanes.[19,20] [b] Dihedral angle constants C_5 and C_6 = 0. All other parameters were adapted from Okada.[22]

Table 3 Charge assignments for the residues of $[MePEG_x\text{-}b\text{-}PCL_y]_6$ star copolymers

Residues[a]	Atoms	Charge/e
Poly(ethylene glycol) (PEG)	O_A	−0.400
	C_B	0.140
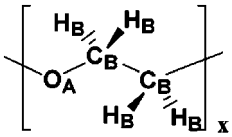	H_B	0.030
Polycaprolactone (PCL)	C_A	0.190
	H_A	0.030
	O_B	−0.330
	C_C	0.510
	C_D	−0.120
	O_E	−0.430
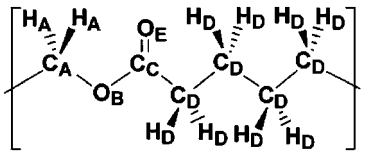	H_D	0.060
Terminal group: CH_2OCH_3	C_A	0.140
	H_A	0.030
	O_B	−0.400
	C_C	0.110
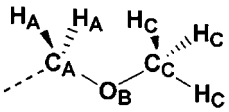	H_C	0.030
Central core: $(CCH_2)_2O$	C_A	0.000
	C_B	0.140
	O_C	−0.400
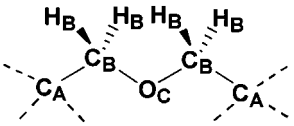	H_B	0.030

[a] The dash bond is the proximal and/or distal end that connects to other residue(s). Charge assignments for the $CH_2OCOOCH_2$ residue (connection fragment between the PEG and PCL) are shown in Table 2.

N_{PCL} : N_{PEG} ratio. The composition and size of each system used in the MD simulations are outlined in Table 1.

2.2 Star-block copolymer parameters

The parameters for Lennard-Jones interactions and Ryckaert–Bellemans dihedrals applied to the $[MePEG_x\text{-}b\text{-}PCL_y]_6$ SCPs are taken from the optimized potentials for liquid simulations (OPLS) parameter set[19,20] and from Charifson *et al.* for PCL ester bond angle.[21] The parameters for the $CH_2OCOOCH_2$ fragment that connects PCL to PEG are adapted from those of dimethyl carbonate[22] as outlined in Table 2. A complete list of SCP charge assignments is included in Table 3. The simple point charge (SPC) water model is used as explicit solvent.[23] Previously, studies have shown that OPLS-AA and other force fields in conjunction with different water models, including SPC and TIP4P, yield free energies of solvation with similar accuracy.[24,25]

2.3 Molecular dynamics simulation protocol

The extended initial coordinates for the $[MePEG_x\text{-}b\text{-}PCL_y]_6$ SCPs are generated using Cerius^2 4.6 software (Accelrys Inc., San Diego, CA.).[26] MD simulations are performed using the leap-frog algorithm for integrating Newton's equations of motion[27] with the GROMACS 3.3.1 simulation software.[28,29] A cubic box containing water and one solute molecule is constructed with an initial minimum distance of 10 Å between the solute and the boundary. The particle-mesh Ewald (PME)[30,31] method is used to calculate the electrostatic interactions every time step with a real-space cutoff of 9 Å. Lennard-Jones interactions are computed using the group-based twin-range cutoff method,[32] calculating interactions every step for separation distances less than 9 Å and every ten steps for separation distances less than 14 Å, when the non-bonded list is updated. The LINCS[33] algorithm is applied to constrain the bond lengths of the solute and the SETTLE[34] algorithm is applied to water molecules to constrain their internal geometry. Following 5000 steps of steepest-descent energy minimization, a short MD simulation is performed in the NPT ensemble at a constant pressure of 1 bar and a temperature of 27 °C, while applying position restraints to the solute. The pressure is controlled isotropically by a Berendsen barostat[35] with a coupling time constant of 4.0 ps^{-1}. To control the temperature, the solute and the solvent are separately coupled to Berendsen thermostats[35] with coupling constants of 0.1 ps^{-1}. Production dynamics are conducted for 200 ns with an integration time step of 2 fs. The coordinates are stored every 10 ps.

2.4 Analysis

Structure. Structural analyses are performed by utilizing analysis tools from GROMACS 4.0.4.[36] The average radius of gyration (R_g) of the hydrophobic PCL core, R_{gcore}, is determined based on all PCL blocks and the dipentaerythriol initiator, whereas the average R_g of the hydrophilic PEG, $R_{gPEGarm}$, is calculated for each PEG arm of the SCP and then averaged. The asphericity index of the hydrophobic PCL core is determined according to the method described by Bruns and Carl[37] (ESI†) where the asphericity index is zero for a perfect sphere and approaches one as the degree of asphericity increases.

Hydration. The spatial range of first hydration shell of PEG is determined based on the first minimum of the radial distribution function (RDF) of all water atoms around the terminal carbon atom of each PEG arm (3.5 Å). The total number of water molecules within the first hydration shell of the six PEG arms excluding the six OCH_3 terminal groups, W_{PEG}, is calculated and then used to determine the average number of water molecules bound per PEG repeat unit (W_{perPEG}). The solvent accessible surface area of the PEG blocks excluding the six OCH_3 terminal groups (A_{PEG}) for the SCPs in aqueous solution is evaluated using the algorithm of Connolly.[38] The average surface area of a water molecule in contact with the polymer, A_{H_2O} (10.2 $Å^2$), is obtained from the A_{PEG} : W_{PEG} ratio for the smallest simulation system. The number of water molecules within 3.5 Å of the PCL core, W_{PCL}, is multiplied by A_{H_2O} in order to obtain the solvent accessed surface area of the PCL core, SAS_{PCL}. Similarly, the solvent accessed surface area of the PEG blocks, SAS_{PEG}, is determined based on W_{PEG} and A_{H_2O}. In cases where a water molecule interacts simultaneously with PEG and PCL polymers, one-half of the interaction is assigned to each polymer. Furthermore, the total solvent accessible surface area of the hydrophobic core (A_{totPCL}) is calculated after removing the PEG blocks and water from the trajectory and then applying the algorithm of Connolly.[38] Therefore, the difference between A_{totPCL} and SAS_{PCL} is the surface area of PCL that is protected from water by the PEG blocks ($A_{protectedPCL}$). It is worth noting that the solvent accessed surface area is the surface area that is

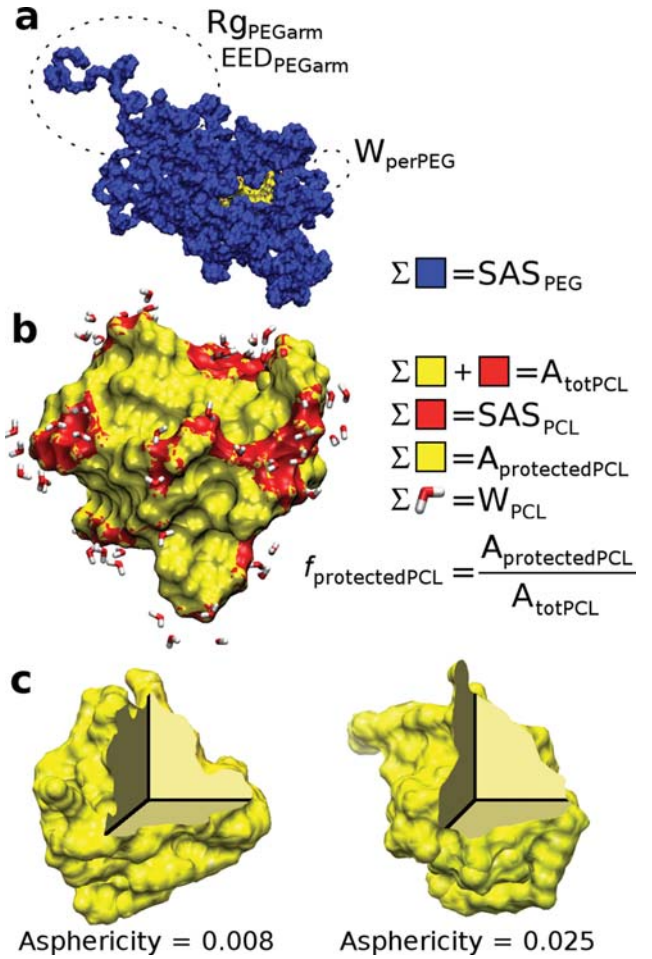

Fig. 1 Summary of properties calculated for $[MePEG_x\text{-}b\text{-}PCL_y]_6$ star copolymers. (a) PEG (blue) is shown partially protecting PCL (yellow). $R_{gPEGarm}$ and EED_{PEGarm} are calculated for each PEG arm and then averaged. SAS_{PEG}, W_{PEG} and R_{gstar} are calculated using the entire SCP. W_{perPEG} is calculated for each PEG repeat unit and then averaged. (b) The PCL core of the SCP is shown without its associated PEG blocks. Water molecules within 3.5 Å of PCL are shown explicitly and counted to yield W_{PCL}. The area of PCL in contact with water (red) is calculated as $SAS_{PCL} = W_{PCL} \times A_{H_2O}$, while the PCL that is successfully protected from water by PEG (yellow) is calculated as $A_{protectedPCL} = A_{totPCL} - SAS_{PCL}$. The total PCL surface area (yellow + red) is represented by A_{totPCL}. The fraction of the PCL surface area that is protected from water by the PEG blocks, $f_{protectedPCL}$, is calculated as $A_{protectedPCL}$ divided by A_{totPCL}. (c) Two PCL cores with different asphericity values are shown to assist the reader interpret this metric.

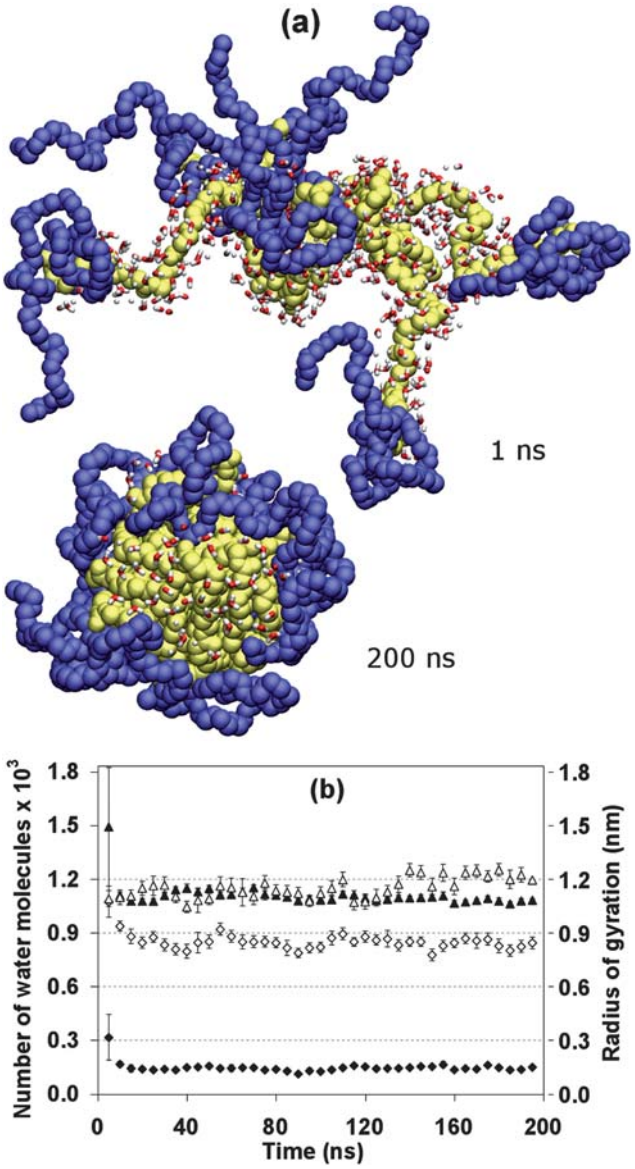

Fig. 2 (a) Snapshot of the $[MePEG_{38}\text{-}b\text{-}PCL_9]_6$ star copolymer at 1 ns and 200 ns highlighting the conformations of PCL (yellow) and PEG (blue) blocks, and water molecules within 3.5 Å of PCL. Bulk water and hydrogen atoms are omitted for clarity. (b) Hydration of PCL core (◆) and PEG blocks (◇) and R_g of PCL core (▲) and PEG blocks (△) of the $[MePEG_{38}\text{-}b\text{-}PCL_9]_6$ star copolymer as a function of simulation time.

actually in contact with water molecules during the simulation, whereas the solvent accessible surface is the area that is available for potential contact by water molecules during simulation and is calculated based on the model developed by Connolly.[38] The various properties calculated for the $[MePEG_x\text{-}b\text{-}PCL_y]_6$ SCPs are outlined in Fig. 1.

3 Results

3.1 Structural properties

Equilibration and convergence. The SCPs investigated in this study are composed of six $MePEG_x\text{-}b\text{-}PCL_y$ arms covalently attached through a small central core, as shown in Table 1. Snapshots of the conformation of $[MePEG_{38}\text{-}b\text{-}PCL_9]_6$ following 1 ns and 200 ns of simulation are shown in Fig. 2a. The hydration of $[MePEG_{38}\text{-}b\text{-}PCL_9]_6$ as a function of simulation time is shown in Fig. 2b. According to W_{PEG} and W_{PCL}, the solvent interaction of the simulated systems is converged after 40 ns (ESI†). Also, 40 ns of simulation are sufficient to converge R_{gcore} and $R_{gPEGarm}$ (ESI†). Generally, during the MD simulations, the PCL blocks quickly collapse and form a compact core within 15 ns. The hydrophilic PEG blocks remain highly hydrated and assume disordered conformations with a high degree of structural heterogeneity.

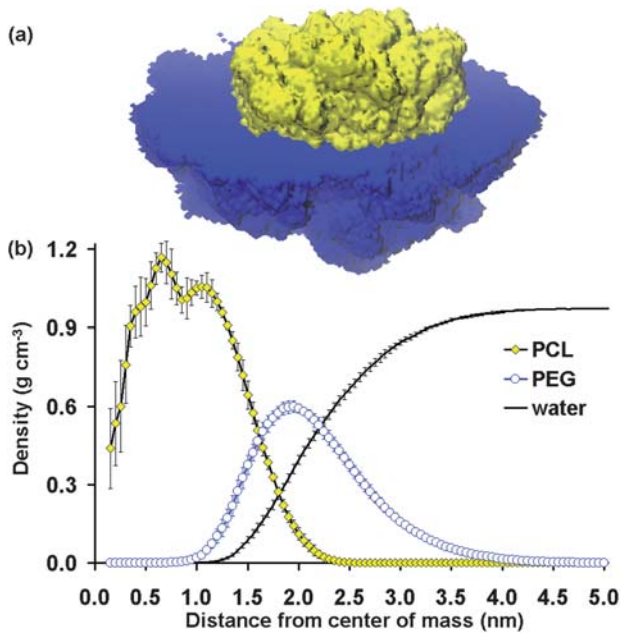

Fig. 3 Spatial distribution of the PCL core and PEG corona in $[MePEG_{113}$-*b*-$PCL_{18}]_6$. (a) Cross-section through a randomly selected but representative snapshot showing the PEG corona (blue) and the PCL core (yellow). (b) Density profile of PCL core (yellow), PEG blocks (blue) and water (black) as a function of distance from the center of mass of the PCL core averaged over the last 160 ns of molecular dynamics simulation.

Self-aggregated structure, size, and shape of PCL. During MD simulations, the PCL blocks form a compact hydrophobic core that preferentially excludes water (data not shown). Concurrently, strong segregation occurs between the hydrophobic PCL core and the hydrophilic PEG corona, as exemplified by the snapshot of $[MePEG_{113}$-*b*-$PCL_{18}]_6$ in Fig. 3a.

Table 4 Asphericity and average radius of gyration of $[MePEG_x$-*b*-$PCL_y]_6$ star copolymers computed from the last 160 ns of the molecular dynamics simulation[a]

				Asphericity $\times 10^{-2}$	
x–*y*	R_{gstar}/Å	$R_{gPEGarm}$/Å	R_{gcore}/Å	PEG	PCL
6–1	9.4 ± 0.3	4.3 ± 0.2 (3.3)	5.8 ± 0.2	9.7 ± 1.1	2.8 ± 0.9
12–2	11.8 ± 0.5	6.3 ± 0.3 (4.9)	7.3 ± 0.4	9.9 ± 1.9	2.5 ± 1.1
19–2	13.5 ± 0.6	8.0 ± 0.4	7.4 ± 0.5	9.3 ± 2.4	4.2 ± 2.4
19–3	13.2 ± 0.6	8.0 ± 0.5 (6.5)	8.2 ± 0.4	9.4 ± 2.4	3.1 ± 1.1
27–2	15.0 ± 0.9	9.7 ± 0.5	7.7 ± 0.3	9.3 ± 2.8	4.9 ± 2.1
27–3	14.9 ± 0.7	9.3 ± 0.6	8.4 ± 0.3	8.2 ± 3.2	2.0 ± 0.8
27–4	14.9 ± 0.7	9.6 ± 0.6 (7.9)	8.7 ± 0.3	8.7 ± 2.7	2.9 ± 1.3
38–3	17.0 ± 0.9	10.8 ± 0.7	8.1 ± 0.4	8.4 ± 2.9	3.0 ± 1.3
38–4	16.6 ± 1.0	11.0 ± 0.5	8.7 ± 0.2	7.8 ± 2.4	2.3 ± 1.0
38–6	16.0 ± 0.6	11.0 ± 0.6	9.9 ± 0.3	8.2 ± 2.6	2.2 ± 0.9
38–9	16.1 ± 0.9	11.5 ± 0.7 (9.7)	10.9 ± 0.5	8.7 ± 2.8	0.8 ± 0.1
113–18	24.1 ± 1.6	16.8 ± 0.7 (18.4)	13.3 ± 0.2	9.3 ± 3.0	0.9 ± 0.5
118–6	26.4 ± 1.6	19.8 ± 0.3 (18.9)	9.7 ± 0.2	6.0 ± 2.6	1.7 ± 0.6

[a] *x* and *y* are the number of repeat units in the PEG and PCL blocks, respectively, of each arm in the $[MePEG_x$-*b*-$PCL_y]_6$ star copolymers. R_{gcore} and R_{gstar} are the radius of gyration of the PCL core (PCL and dipentaerythriol initiator) and entire star copolymer, respectively. $R_{gPEGarm}$ is the average radius of gyration of each PEG arm. Values in parentheses are the radii of gyration for the PEG blocks calculated based on Flory's model,[55,56] $R_{gFloryPEG} = (a/\sqrt{6})N_{PEG}^{\alpha}$, where $a = 2.8$ Å for PEG[57] and $\alpha = 0.588$ for polymer in good solvent.

Importantly, self-organization of the hydrophobic PCL core is observed. The hydrophobic cores of SCPs with $N_{PCL} \geq 9$ (*i.e.* with $y = 9$ or 18) are relatively spherical, having an asphericity index of $\leq 0.009 \pm 0.001$ (Table 4). As N_{PCL} decreases, the shape of the hydrophobic core shifts towards an ellipsoid where the asphericity index of the core ranges from 0.017 to 0.049 as shown in Table 4. Amongst the different systems, the interior hydrophobic PCL core becomes more densely packed with increasing total M_{wPCL} and reaches a density of 1.1 to 1.2 g cm^{-3} at a distance of 4 Å from the center of mass (COM) of the hydrophobic core (ESI†).

As shown in Fig. 4a, the average R_{gcore} can be described as a function of N_{PCL} according to the following equation:

$$R_{gcore} = 6.05 N_{PCL}^{0.273} \text{ (Å)} \ (R^2 = 0.986) \quad (1)$$

Transition phase between PCL and PEG. There exists a distance from the COM of the core at which the density of PCL equals that of PEG, generally in the presence of a small but reproducible amount of water (Fig. 3b). This represents the most likely distance from the COM of the core at which an amphiphilic transition phase exists between the dominantly hydrophobic and hydrophilic regions of the aggregated copolymer. The apparent thickness of this transition (Fig. 3b) is an artifact that results from radially averaging an imperfect spherical object. The environmental transition is nearly discrete when instantaneous snapshots are assessed (Fig. 3a).

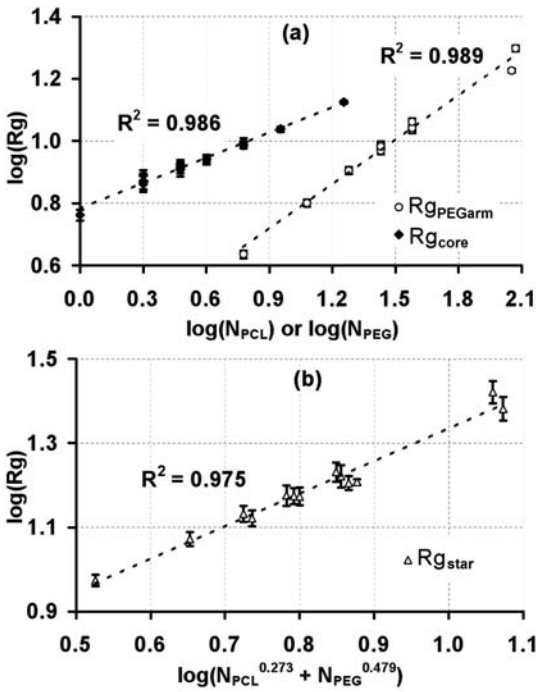

Fig. 4 Double-logarithmic scales of the mean radius of gyration of (a) the PCL core (R_{gcore}) *versus* N_{PCL} (●), the PEG block ($R_{gPEGarm}$) *versus* N_{PEG} (○) and (b) the entire star copolymer (R_{gstar}) *versus* sum of $N_{PCL}^{0.273}$ and $N_{PEG}^{0.479}$ for $[MePEG_y$-*b*-$PCL_x]_6$ star copolymers. Data are computed from the last 160 ns of the molecular dynamics simulations. The dashed lines are the linear fit functions. The radius of gyration is expressed in Å.

Conformation, size, and extension of PEG. In contrast to PCL, the PEG blocks are highly hydrated during the MD simulation, and thus the PEG corona is significantly less densely packed than the hydrophobic PCL core (Fig. 3b). As such, the PEG corona occupies a significantly larger volume than the core. For all SCPs investigated in the current study, the MD simulations reveal that the PEG blocks move rapidly and are globally disordered while transiently adopting a local helical structure with 3.5 PEG repeat units per turn (data not shown). For SCPs with $N_{PEG} \geq 19$, the distal ends of the PEG blocks either extend away from the proximal ends, or curl back to form a Gaussian coil providing partial shielding of the hydrophobic core from solvent as shown in the trajectory of $[MePEG_{113}\text{-}b\text{-}PCL_{18}]_6$ (Trajectory movie†). For SCPs with shorter PEG chains, the ends of all PEG blocks remain extended, with a median EED_{PEGarm} of 8.0 ± 0.1 Å ($N_{PEG} = 6$) and 10.5 ± 0.1 Å ($N_{PEG} = 12$) as shown in ESI†. The conformation of PEG in the corona is also measured by the R_g of each PEG arm, $R_{gPEGarm}$. A linear relationship is obtained for $R_{gPEGarm}$ as a function of N_{PEG} (Fig. 4a), allowing $R_{gPEGarm}$ to be predicted using the following relationship:

$$R_{gPEGarm} = 1.93 N_{PEG}^{0.479} \text{ (Å)} \ (R^2 = 0.989) \quad (2)$$

As shown in Fig. 4b, the size of the SCP is more strongly related to N_{PEG} than to N_{PCL} and can be determined based on the relationship between the R_g of the entire SCP, R_{gstar}, and the total degree of polymerization of the PEG and PCL blocks as shown in eqn (3) (Table 4 and Fig. 4b).

$$R_{gstar} = 3.59(N_{PEG}^{0.479} + N_{PCL}^{0.273})^{0.780} \text{ (Å)} \ (R^2 = 0.975) \quad (3)$$

3.2 Solvation properties

Hydration and solvent accessible surface area of PCL. MD simulation of SCPs in explicit water allows the calculation of the number of water molecules in the first hydration shell (within 3.5 Å) of the polymers. A snapshot of the $[MePEG_{38}\text{-}b\text{-}PCL_9]_6$ SCP highlighting the interaction of the hydrophobic PCL core with water at a simulation time of 200 ns is shown in Fig. 1b. Once the PCL component exceeds a total M_{wPCL} of 2.05 kDa ($N_{PCL} = 3$), the interior of the hydrophobic core is completely devoid of water (data not shown). Importantly, the number of water molecules bound to the surface of the hydrophobic PCL core, W_{PCL}, is found to depend on both N_{PCL} and N_{PEG}. In particular, W_{PCL} decreases with an increase in N_{PEG} when N_{PCL} is held constant, as shown in Table 5. The quantification of this relationship, as described below, is one of the major results in this study, and is an essential step towards the rational design of unimolecular SCP micelles.

A collective analysis of these simulations reveals that the total solvent accessible surface area of the hydrophobic PCL core, calculated by the algorithm of Connolly[38] after excluding the PEG blocks, A_{totPCL}, can be predicted according to eqn (4). A linear relationship is obtained between N_{PCL} and A_{totPCL}, as shown in Fig. 5a.

$$A_{totPCL} = 364(6N_{PCL})^{0.627} \text{ (Å}^2\text{)} \ (R^2 = 0.991) \quad (4)$$

As expected, A_{totPCL} depends only on N_{PCL}, whereas the surface area of PCL that is protected from water by the PEG block, $A_{protectedPCL}$, is significantly influenced by the PEG blocks such that an increase in N_{PEG} results in an increase in $A_{protectedPCL}$ (Table 5). Significantly, our results quantify the increase in the fraction of the hydrophobic core protected from water by PEG, $f_{protectedPCL}$, with an increase in N_{PEG} (Fig. 5b), where $f_{protectedPCL}$ is the ratio of $A_{protectedPCL}$ to A_{totPCL}:

$$f_{protectedPCL} = 0.228\log(6N_{PEG}) + 0.245 \ (R^2 = 0.933) \quad (5)$$

Hydration of PEG. As shown in Table 5, large hydration values for PEG blocks, W_{PEG}, are obtained for all SCPs, demonstrating a high solubility for PEG in water. Furthermore, the average hydration number of PEG, W_{PEG}, increases linearly with an increase in N_{PEG} (Table 5 and Fig. 5c). This yields a theoretical description of W_{PEG} that can be expressed as:

Table 5 Solvation properties for the PEG and PCL blocks of star copolymers computed from the last 160 ns of the molecular dynamics simulation[a]

x–y	W_{PEG}[b]	$W_{PCL/PEG}$	W_{PCL}	SAS_{PEG}/Å^2	SAS_{PCL}/Å^2	A_{totPCL}/Å^2	$A_{protectedPCL}$[c]/Å^2	$f_{protectedPCL}$
6–1	177 ± 6 (4.9)	32 ± 2	43 ± 2	1888 ± 74	461 ± 23	1129 ± 31	669 ± 38	0.59 ± 0.04
12–2	317 ± 11 (4.4)	45 ± 3	57 ± 4	3366 ± 140	614 ± 44	1689 ± 69	1075 ± 82	0.64 ± 0.06
19–2	467 ± 23 (4.1)	45 ± 4	46 ± 4	4968 ± 268	488 ± 43	1704 ± 63	1216 ± 76	0.71 ± 0.05
19–3	448 ± 23 (3.9)	55 ± 4	62 ± 5	4762 ± 271	657 ± 52	2169 ± 68	1512 ± 101	0.70 ± 0.05
27–2	616 ± 27 (3.8)	49 ± 7	39 ± 5	6550 ± 310	418 ± 57	1871 ± 67	1453 ± 88	0.78 ± 0.06
27–3	611 ± 27 (3.8)	57 ± 6	53 ± 5	6498 ± 313	559 ± 55	2444 ± 77	1885 ± 95	0.77 ± 0.05
27–4	617 ± 37 (3.8)	62 ± 5	60 ± 5	6559 ± 431	640 ± 48	2564 ± 76	1924 ± 90	0.75 ± 0.04
38–3	860 ± 40 (3.8)	53 ± 6	38 ± 4	9146 ± 449	405 ± 45	2143 ± 82	1738 ± 93	0.81 ± 0.05
38–4	816 ± 45 (3.6)	62 ± 8	47 ± 6	8679 ± 501	500 ± 67	2606 ± 75	2106 ± 101	0.81 ± 0.05
38–6	797 ± 40 (3.5)	82 ± 8	64 ± 6	8476 ± 467	682 ± 64	3421 ± 112	2740 ± 129	0.80 ± 0.05
38–9	794 ± 29 (3.5)	99 ± 8	93 ± 4	8445 ± 322	988 ± 79	4359 ± 112	3371 ± 165	0.77 ± 0.04
113–18	2206 ± 124 (3.3)	138 ± 9	88 ± 6	23 468 ± 1329	932 ± 63	7239 ± 168	6307 ± 179	0.87 ± 0.03
118–6	2495 ± 107 (3.5)	69 ± 8	40 ± 4	26 533 ± 1166	442 ± 47	3292 ± 109	2868 ± 119	0.87 ± 0.05

[a] x and y are the number of repeat units in the PEG and PCL blocks, respectively, for each arm of $[MePEG_x\text{-}b\text{-}PCL_y]_6$. W_{PEG} and W_{PCL} are the number of water molecules within 3.5 Å of the PEG and PCL blocks, respectively. $W_{PCL/PEG}$ is the number of water molecules that interact with PEG and PCL simultaneously. SAS_{PEG} and SAS_{PCL} are the total solvent accessed surface areas of PEG and PCL, respectively. A_{totPCL} is the total solvent accessible surface area of PCL. [b] Values in parentheses are number of water molecules per repeat unit. [c] The surface area of PCL protected by PEG calculated based on MD simulation: $A_{protectedPCL} = A_{totPCL} - SAS_{PCL}$; $f_{protectedPCL} = A_{protectedPCL}/A_{totPCL}$ represents the fraction of the PCL core protected from water.

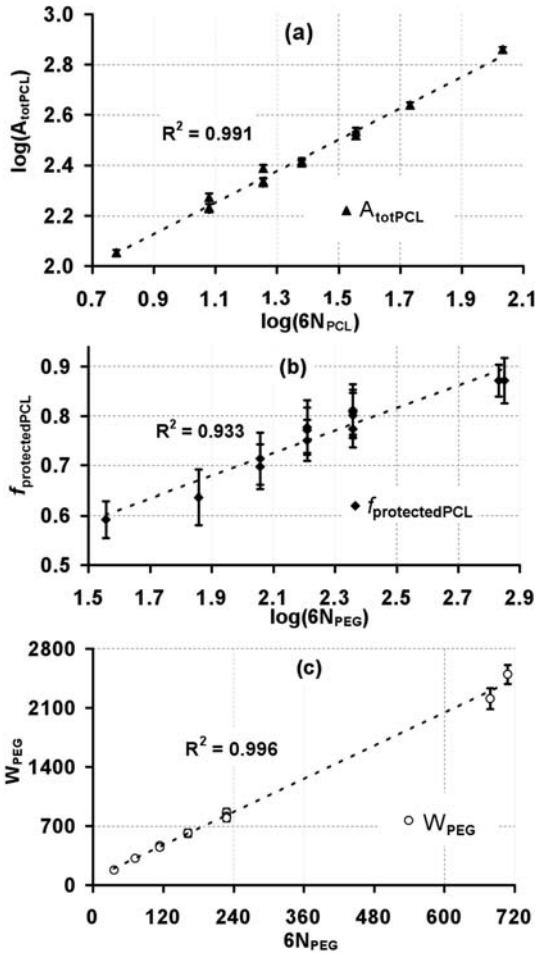

Fig. 5 Solvation properties of various star copolymers, obtained by calculating the number of water molecules within 3.5 Å of the polymers. (a) Double-logarithmic scales of total surface area of PCL core assuming zero protection by PEG *versus* the total number of PCL units. (b) Fraction of PCL at the core surface that is protected from water by PEG, $f_{protectedPCL}$, *versus* a logarithmic scale of the total number of PEG units. (c) Hydration of the PEG corona *versus* the total number of PEG units. Data are evaluated from the last 160 ns of the molecular dynamics simulations. The dashed lines are the linear fit functions.

$$W_{PEG} = 3.3(6N_{PEG}) + 74(\text{molecules}) \ (R^2 = 0.996) \qquad (6)$$

For the various SCPs in this study, the average number of water molecules predicted to bind per PEG repeat unit, W_{perPEG}, ranges from 3.3 to 4.9 (Table 5). As well, the average W_{perPEG} is independent of the PCL block length for all SCPs (eqn (6) and Fig. 5c).

4 Discussion

4.1 Validation of simulation parameters

The current MD simulations reproduce the known aqueous properties of PCL-*b*-PEG blocks copolymers,[39,40] wherein the hydrophobic PCL core is largely dehydrated and solvated by a water soluble PEG corona (Fig. 3a). These fundamental properties emerge from the simulations in spite of the fact that the force fields that are employed do not contain any special terms that dictate solubility explicitly. Rather, hydrophobic collapse in these simulations is driven by the same forces that exist in a test tube, namely the entropically disfavoured formation of an aqueous solvation shell around a non-polar solute. This is consistent with the success of all-atom force fields in computing the self-organization of other micelle-forming molecules, such as detergents,[41] as well as the formation of lipid bilayers.[42]

Structure and dehydration of the PCL core. The aggregated structure of the PCL core that emerges from MD simulations agrees well with the known properties of this polymer (*e.g.* water insoluble), confirming that our simulations are sampling the relevant phase of this polymer. In particular, the PCL blocks form a compact hydrophobic core that excludes water and PEG (Fig. 3a).

The linear relationship between R_{gcore} and N_{PCL} for all simulated systems (eqn (1)) indicates a similar packing pattern and architecture for PCL within the hydrophobic cores of all SCPs. For $N_{PCL} \geq 4$, the partial overlap of the radial density of PCL and water that is apparent in Fig. 3b is not the result of actual coexistence. Rather it is an artifact of the radial averaging of an inherently aspherical hydrophobic PCL core (Table 4). The same is true for PCL and PEG, which do not mix, beyond the close interactions of two rough interfaces. For $N_{PCL} \leq 3$, however, the exclusion of water from the PCL core is incomplete. Many studies have proposed that the presence of water at the PCL–PEG interface of micelles promotes hydrolytic degradation of the core, for example, by ester bond cleavage within the PCL blocks.[43] Further, an increase in the rate of degradation of PCL with decreasing M_w has been reported based on dynamic light scattering, nuclear magnetic resonance and gel permeation chromatography measurements for $MePEG_x$-*b*-PCL_y ($x = 117$, $y = 7$, 13 and 17) linear diblock copolymer micelles[44] and 3-arm $(PEG_{136}$-*b*-$PCL_y)_3$ SCP micelles ($y = 11$, 18 and 30).[45] In the current study, therefore, the presence of water in the interior of the PCL core for $N_{PCL} \leq 3$ suggests that SCPs with $N_{PCL} \leq 3$ may degrade more quickly than SCPs with larger N_{PCL}.

Hydration of the PEG corona. The present study provides a detailed measurement of polymer hydration at the atomistic level with systematic exploration of polymer M_w and conformation (Table 5 and Fig. 5c). Eqn (6) allows prediction of the hydration of PEG of a known M_w within the range of 0.3 kDa to 5.2 kDa, which encompasses the PEG polymers employed for numerous biomedical applications.[46] These results are consistent with the known unlimited solubility of PEG in water[47–49] (Fig. 5c), which has been suggested to be due to hydrogen bonding between the ether oxygen of the polymer and water.[50] Furthermore, for SCPs with long PEG chains there is an increased probability that water molecules may form a hydrogen bonding "bridge" between PEG arms or PEG repeat units (ESI†). Such water bridges have been found previously using ^1H and ^2H nuclear magnetic resonance measurements for 6 kDa PEG ($N_{PEG} = 136$) in low water content.[51] In the current study, the decrease in W_{perPEG} values that occurs with an increase in N_{PEG} from 6 ($W_{perPEG} = 4.9$) to 118 ($W_{perPEG} = 3.5$) is indicative

of the replacement of the water–PEG interactions by PEG–water–PEG and/or PEG–PEG interactions (Table 5).

As shown in Table 5, the average W_{perPEG} obtained from the current study decreased from 4.9 to 3.3 when the N_{PEG} increased from 6 to 118. In comparison, experimental evaluation of PEG of varying M_w has yielded estimates of W_{perPEG}, with values ranging from 1.0 to 5.0 for linear PEG chains with N_{PEG} in a range of 4.5 to 182.[49,51,52] Indeed the estimates obtained experimentally for W_{perPEG} for PEG of similar molecular weights have been quite variable.[49,51–53] For example, Branca *et al.* reported a linear relationship between the degree of hydration of linear PEG and M_{wPEG} with W_{perPEG} values increasing from 2.2 to 5.0 when N_{PEG} increased from 4.5 to 45, based on viscosity measurements.[53] Ng and Rosenberg found the minimum W_{perPEG} to be 2.5, as determined by measuring the heat capacity for the interaction between water and 8 kDa PEG (N_{PEG} = 182).[49] A nuclear magnetic resonance spectroscopy study of 6 kDa PEG (N_{PEG} = 136) by Lusse and Arnold suggested that there is a maximum of one water molecule in contact with a single PEG monomer unit.[51]

As reviewed by Allen *et al.*,[47] the variation in the number of water molecules reported to interact with a single PEG repeat unit may be attributed to differences in PEG conformation which depends largely on M_{wPEG}, the architecture of the polymer and the environment (*e.g.* temperature, concentration, surface tethering, and surface density). In this regard, Tirosh *et al.* proposed that the conformations of 2 kDa PEG grafted to liposomes and free in solution are brush ($W_{perPEG} \approx 4.6$) and random coil ($W_{perPEG} \approx 3.0$), respectively.[52] In another study, it was found that the degree of water uptake depends on the architecture of the SCP such that increasing the number of arms results in a decrease in hydration as determined by gravimetric analysis of copolymer films.[54] Furthermore, the instruments used to measure the hydration of PEG can affect the hydration results. For example, the W_{perPEG} values ($N_{PEG} \approx 4.5$ to 45) obtained by acoustic measurements (1.6 to 2.3) are smaller than those determined by viscosity measurements (2.2 to 5.0).[53] Importantly, the W_{perPEG} values obtained from the current study directly quantify the number of water molecules that are in contact with the PEG blocks.

4.2 Relationship to other theoretical and simulation models

Previously, Flory put forth the "random flight" model to predict the size of linear polymers in terms of the R_g.[55,56] In the current study, the size of the PEG chain can be expressed in terms of the R_g based on Flory's theory, $R_{gFloryPEG} = a/\sqrt{6}N_{PEG}^{\alpha}$ (ESI†) where a is the size of one PEG repeat unit (a = 2.8 Å[57]) and α is a unitless coefficient describing the compatibility of the polymer and solvent. As shown in Fig. 4a, the linear fits from the plot of M_{wPEG} as function of $R_{gPEGarm}$ on a double-logarithmic scale yield an α value of 0.479 for the PEG blocks in water (eqn (2)). This result is similar to the α value for a θ solvent (α = 0.5) in which the polymer is said to behave ideally and exist in a Gaussian coil. However, the α value obtained for the PEG blocks from the current study was smaller than the experimental α values obtained for linear PEG in water with 0.2 kDa < M_{wPEG} < 7.5 kDa (α = 0.523)[58] and for single-chain poly(ethylene oxide) (PEO) in water with 25 kDa < M_{wPEO} < 100 kDa (α = 0.583).[59] Furthermore, the current study found that the PEG blocks of the SCPs absorbed to the surface of the PCL core. As can be calculated from data in Table 4, the percent difference between the radii of gyration calculated based on Flory theory, $R_{gFloryPEGarm}$ (ESI†), and $R_{gPEGarm}$ obtained from the current study decreases from 23% to 5% as N_{PEG} increases from 6 to 118. Recently, a spherical micelle formed from PEG_{11}-*b*-poly(γ-benzyl L-glutamate)$_9$ linear diblock copolymer was studied by all-atom MD for a total simulation time of 7 ns.[60] In order to achieve longer simulation times, Lee *et al.* parameterized linear PEG[61] into the MARTINI coarse-grained (CG) force field[62] based on all-atom simulation of linear PEG with 9 ≤ N_{PEG} ≤ 37.[63] From these studies, radii of gyration of PEG comparable with experimental values were obtained having α values of 0.51 and 0.515 for 9 ≤ N_{PEG} ≤ 37,[61,63] and an α value of 0.57 for 36 < N_{PEG} ≤ 158.[61] In a follow up study based on the MARTINI parameterization of linear PEG,[18] CG simulations of dendrimers composed of PEG–polyamidoamine in water reveal that the PEG blocks (0.55 to 5 kDa) of a densely grafted dendrimer extend outward from the core and stabilize nanoparticles preventing their aggregation.[18] In these studies, the authors noted that the spatial extension of the PEG corona, brush on a hydrophobic surface, agreed with experimental measurement and with theoretical predictions from de Gennes theory.[18] Nevertheless, it should be noted that CG parameters are context dependent. It is unclear if CG parameters developed from atomistic simulations of PEG in water are applicable to the simulation of $MePEG_x$-*b*-PCL_y in the context of a SCP. Importantly, our results discern the hydrophobic behavior of the SCPs in water and can be employed to parameterize $MePEG_x$-*b*-PCL_y SCPs into CG models.

In comparison to theoretical[18,61,63] and experimental studies[58,59] that have examined the radius of gyration of PEG, the α value (0.479) obtained from our simulations is smaller indicating that the PEG blocks are more compact in the context of SCPs. This discrepancy may be attributed to the difference in M_w of the PEG blocks relative to the PCL core and architecture of the copolymer. The conformation of polymers grafted to a curved surface has theoretically been predicted to be dependent on the chain length of the polymer and the radius of curvature.[64] Specifically, when the ratio of the radius of curvature and the thickness of the grafted polymer layer ≪ 1, the R_g of the grafted polymers grows as a function of the degree of polymerization of the polymer with α equal to 3/5.[64] Further, the theoretical model developed by Daoud and Cotton showed that the radius of a star shaped polymer is smaller than that of a linear polymer of the same M_w.[65]

4.3 Quantification of hydration of the PCL core as a predictor for multimolecular aggregation

Although considerable effort has been expended both theoretically and experimentally to describe the effect of hydration on the macromolecular structure and stability of MePEG-*b*-PCL micelles formed by SCPs or linear diblock copolymers,[40,48,52,66–70] quantification of the number of water molecules that interact with PCL has remained elusive. For the first time we present a detailed molecular model quantifying the number of water molecules that interact with the hydrophobic PCL core of

various six-arm SCPs. Based on our analysis, the solvent accessed surface area of the hydrophobic PCL core depends not only on the surface area and aggregated structure of the copolymer, but also on the length and conformation of the PEG blocks, whereby increasing PEG block length reduces the exposure of the PCL core to the aqueous environment (Table 5 and Fig. 5b). The W_{PCL} values presented in Table 5, however, demonstrate that none of the SCPs in this study contain a PEG corona that is capable of providing full coverage of the hydrophobic core, exposing segments of the PCL core to water.

In a concentrated aqueous solution of SCPs, the unshielded PCL units would also be in potential contact with PCL units of another unimer, a potential interaction that is highly relevant to self-aggregation. Nevertheless, it is unknown whether the formation of multimolecular micelles is due in part to core–core interaction and/or entanglement of PEG chains of different SCPs. Investigation of aggregation of multiple SCPs is currently in progress in order to better understand the interactions that drive this process. We postulate that the propensity for aggregation of SCPs is correlated with the fractional hydration of the hydrophobic PCL core in the unimolecular state, which is found to vary from 46% to 23% for the SCPs investigated in this study depending on the M_w of the PCL and PEG blocks (Table 5 and Fig. 5b). Sufficient water-exposed surface area of the non-polar PCL blocks may destabilize the unimolecular state and thus drive intermolecular association between SCPs resulting in the formation of multimolecular micelles in aqueous media. Accordingly, multimolecular micelles of SCPs with a M_w similar to [MePEG$_{113}$-*b*-PCL$_{18}$]$_6$ are observed by dynamic light scattering and transmission electron microscopy at a copolymer concentration of 3.4×10^{-6} mol L^{-1} in water (F. Li and C. Allen, unpublished results). Significantly, the results of the present study are highly quantitative and, as such, may be utilized to rationally design a SCP with a hydrophobic core that is sufficiently protected from water such that it may exclusively form stable unimolecular micelles.

4.4 Rational design of unimolecular micelles

Aggregation between SCPs is likely to result from interactions between water-exposed-PCL segments. The quantitative results of the present study predict the optimal ratio(s) of N_{PCL} to N_{PEG} for a SCP in order to minimize the hydration of the PCL core. In particular, extrapolation of eqn (5) for maximum protection of the PCL core ($f_{protectedPCL} = 1$) dictates the minimum N_{PEG} ($N_{PEG} = 336$ and $M_w = 14.8$ kDa) that is required to completely cover the PCL core. Interestingly, the requisite N_{PEG} is independent of N_{PCL} within the confidence interval ($N_{PCL} \leq 18$, $4.2 \leq N_{PEG}/N_{PCL} \leq 19.7$, Table 1). The hypothetical SCP [MePEG$_{336}$-*b*-PCL$_{18}$]$_6$ has a PCL core that we predict is fully protected from solvent and has a predicted R_{gcore} and $R_{gPEGarm}$ of 13.3 Å and 31.3 Å obtained by utilizing eqn (1) and (2), respectively. Indeed, PEG blocks of this M_w have been employed to stabilize diblock copolymer micelle formulations.[46,71] Importantly, the stability predicted by eqn (5) is thermodynamic, distinct from any kinetic stability[72,73] that may be afforded by a large PEG corona.

It is important to emphasize that much of the information gained from the MD simulations cannot be obtained by performing experimental studies on the individual SCPs examined in the present study. Experimentally, these SCPs are likely to aggregate in solution, whereas our simulations sample the conformations adopted by unimers at infinite dilution. This allows us to fully characterize the unimolecular state and not only identify the source of thermodynamic instability, but also to quantify the source of instability and thereby predict stable unimolecular compositions. The significance of the present study is the elucidation of quantitative relationships that are instrumental in the rational design of SCPs. The size of the SCP is more strongly related to N_{PEG} than to N_{PCL} (Table 4), and it is, in many cases, undesirable to increase the size of the unimolecular micelle *ad infinitum* in order to achieve complete protection of the hydrophobic PCL core from solvent. The quantitative results of this study indicate the minimal size at which the hydrophobic PCL core can be completely protected from water.

4.5 Alternative SCP architectures

It remains to be experimentally confirmed whether PEG can completely protect the hydrophobic PCL core of six-armed diblock star copolymers, since the water molecules that interact with PEG at the PEG–PCL interface can also interact with PCL. Regardless of PEG length, there is either a small amount of water interacting with the hydrophobic core or a small amount of proximal PEG that is unfavourably dehydrated. Inclusion of an amphiphilic block between the hydrophobic and hydrophilic blocks may be desirable in some cases.

Furthermore, the architecture of the SCP may need to be modified in combination with optimization of the ratio of the PEG and PCL block lengths. As well, the chemical structure of the central connector may need to be considered in order to utilize the relationship between the structural properties and M_w of the PCL core for other SCPs that have chemically different connectors. Recently, Schramm *et al.* synthesized many SCPs having 4 and 6 arm PCL$_{12}$ cores ($N_{PCL} = 12$) that are conjugated to 4-, 6-, 8- and 12-branched-PEG ($N_{PEG} = 8$ to 30) per PCL arm.[12] Interestingly, these SCPs behave as unimolecular micelles according to dynamic light scattering measurements. Nevertheless, simply increasing the number of arms of the SCP does not necessarily result in a unimolecular micelle. For example, a previous experimental study revealed that (MePEG$_{113}$-*b*-PCL$_{26}$)$_{16}$ SCPs formed multimolecular micelles (CMC of *ca.* 3 mg mL^{-1}).[9]

5 Conclusions

Our simulations elucidate the solution behavior of [MePEG$_x$-*b*-PCL$_y$]$_6$ SCPs in water and predict a densely packed hydrophobic core that is phase separated from a highly mobile hydrophilic PEG corona. The average number of water molecules predicted to bind per PEG repeat unit is in the range of 3.3 to 4.9, in good agreement with experimental data for SCPs with high M_{wPEG}. The conformation of the hydrophobic PCL core and the conformational and solution properties of the PEG shell are predictable and independent of the ratio of hydrophilic to hydrophobic block length. This report reveals that, with the PCL and PEG composition investigated in this study, the PEG corona of six-armed diblock SCPs provides only partial coverage of the

hydrophobic core, leaving segments of PCL exposed to water. Although it is likely that a simple increase in the amount of PEG will be sufficient to entirely encapsulate the PCL core and protect the SCPs from PCL mediated aggregation, the M_w of the SCP also needs to be sufficiently small for utilization of the material for a particular application (*e.g.* drug delivery). Unique to this study, the hydration of the PCL core is quantified as a function of N_{PCL} and N_{PEG}, enabling prediction of the minimum N_{PEG} required for complete protection of a core with a specific M_{wPCL}. Overall, this study provides fundamental insight into the properties of star copolymers in aqueous solution that should be useful for rationally designing a second generation of star copolymers that exclusively form unimolecular micelles. In addition, the systematic methodology developed in this study is applicable to the design of arbitrarily composed polymers for which the principle requirement is the protection of a hydrophobic surface from aqueous solution.

Acknowledgements

This study is supported by a grant from NSERC to C. Allen as well as a University of Toronto Open Fellowship to L. Huynh. C. Neale is funded by the Research Training Center at the Hospital for Sick Children and by the University of Toronto. The authors are grateful to the Centre for Computational Biology High Performance Facility (CCBHPF) at the Hospital for Sick Children (Toronto, ON) and the Shared Hierarchical Academic Research Computing Network (SHARCNET) for generous allocations of computational resources (Toronto, ON). R. Pomès is a CRCP Chairholder. L.H. thanks Fugang Li for synthesizing and characterizing the $[MePEG_{113}$-*b*-$PCL_{18}]_6$ SCP.

References

1 N. Kumar, M. N. V. Ravikumar and A. J. Domb, *Adv. Drug Delivery Rev.*, 2001, **53**, 23–44.
2 C. J. Allen, *J. Liposome Res.*, 2003, **13**, XI–XII.
3 E. Lavik and R. Langer, *Appl. Microbiol. Biotechnol.*, 2004, **65**, 1–8.
4 R. C. Eberhart, S. H. Su, K. T. Nguyen, M. Zilberman, L. Tang, K. D. Nelson and P. Frenkel, *J. Biomater. Sci., Polym. Ed.*, 2003, **14**, 299–312.
5 S. Forster and M. J. Konrad, *J. Mater. Chem.*, 2003, **13**, 2671–2688.
6 A. Heise, J. L. Hedrick, C. W. Frank and R. D. Miller, *J. Am. Chem. Soc.*, 1999, **121**, 8647–8648.
7 A. B. Nguyen, N. Hadjichristidis and L. J. Fetters, *Macromolecules*, 1986, **19**, 768–773.
8 G. Mountrichas, M. Mpiri and S. Pispas, *Macromolecules*, 2005, **38**, 940–947.
9 F. Wang, T. K. Bronich, A. V. Kabanov, R. D. Rauh and J. Roovers, *Bioconjugate Chem.*, 2005, **16**, 397–405.
10 H. Lee, F. Zeng, M. Dunne and C. Allen, *Biomacromolecules*, 2005, **6**, 3119–3128.
11 F. Wang, T. K. Bronich, A. V. Kabanov, R. D. Rauh and J. Roovers, *Bioconjugate Chem.*, 2008, **19**, 1423–1429.
12 O. G. Schramm, G. M. Pavlov, H. P. van Erp, M. A. R. Meier, R. Hoogenboom and U. S. Schubert, *Macromolecules*, 2009, **42**, 1808–1816.
13 M.-C. Jones, M. Ranger and J. C. Leroux, *Bioconjugate Chem.*, 2003, **14**, 774–781.
14 M. Liu, K. Kono and J. M. J. Frechet, *J. Controlled Release*, 2000, **65**, 121–131.
15 J. Xin, D. Liu and C. Zhong, *J. Phys. Chem. B*, 2007, **111**, 13675–13682.
16 Y. Chang, W.-C. Chen, Y.-J. Sheng, S. Jiang and H.-K. Tsao, *Macromolecules*, 2005, **38**, 6201–6209.
17 F. Ganazzoli, Y. A. Kuznetsov and E. G. Timoshenko, *Macromol. Theory Simul.*, 2001, **10**, 325–338.
18 H. Lee and R. G. Larson, *J. Phys. Chem. B*, 2009, **113**, 13202–13207.
19 W. L. Jorgensen, *OPLS, Force Field. Encyclopedia of Computational Chemistry*, Wiley, New York, 1998, vol. 3, pp. 1986–1989.
20 W. L. Jorgensen, D. S. Maxwell and J. Tirado-Rives, *J. Am. Chem. Soc.*, 1996, **118**, 11225–11236.
21 P. S. Charifson, R. G. Hiskey and L. G. Pedersen, *J. Comput. Chem.*, 1990, **11**, 1181–1186.
22 O. Okada, *Mol. Phys.*, 1998, **93**, 153–158.
23 H. J. C. Berendsen, J. P. M. Postma, W. F. van Gunsteren and J. Hermans, Interaction Models for Water in Relation to Protein Hydration, in *Intermolecular Forces*, ed. B. Pullman, 1981, Reidel, Dordrecht, The Netherlands.
24 J. L. MacCallum and D. P. Tieleman, *J. Comput. Chem.*, 2003, **24**, 1930–1935.
25 B. Hess and N. F. van der Vegt, *J. Phys. Chem. B*, 2006, **110**, 17616–17626.
26 K. J. Volk, S. E. Hill, H. E. Kerns and M. S. Lee, *J. Chromatogr., B: Biomed. Sci. Appl.*, 1997, **696**, 99–115.
27 R. W. Hockney, S. P. Goel and J. Eastwood, *J. Comput. Phys.*, 1974, **14**, 148–158.
28 H. J. C. Berendsen, D. van der Spoel and R. van Drunen, *Comput. Phys. Commun.*, 1995, **91**, 43–56.
29 E. Lindahl, B. Hess and D. van der Spoel, *J. Mol. Model*, 2001, **7**, 306–317.
30 T. Darden, D. York and L. Pedersen, *J. Chem. Phys.*, 1993, **98**, 10089–10092.
31 U. Essmann, L. Perera, M. L. Berkowitz, T. Darden, H. Lee and L. G. Pedersen, *J. Chem. Phys.*, 1995, **103**, 8577–8592.
32 W. F. van Gunsteren and H. J. C. Berendsen, *Angew. Chem., Int. Ed. Engl.*, 1990, **29**, 992–1023.
33 B. Hess, H. Bekker, H. J. C. Berendsen and J. G. E. M. Fraaije, *J. Comput. Chem.*, 1997, **18**, 1463–1472.
34 S. Miyamoto and P. A. Kollman, *J. Comput. Chem.*, 1992, **13**, 952–962.
35 H. J. C. Berendsen, J. P. M. Postma, W. F. van Gunsteren, A. D. Nola and J. R. Haak, *J. Chem. Phys.*, 1984, **81**, 3684–3691.
36 B. Hess, C. Kutzner, D. van der Spoel and E. Lindahl, *J. Chem. Theory Comput.*, 2008, **4**, 435–447.
37 W. Bruns and W. Carl, *Macromolecules*, 1991, **24**, 209–212.
38 M. Connolly, *Science*, 1983, **221**, 709–713.
39 C. Allen, Y. Yu, D. Maysinger and A. Eisenberg, *Bioconjugate Chem.*, 1998, **9**, 564–572.
40 C. Lu, L. Liu, S.-R. Guo, Y. Zhang, Z. Li and J. Gu, *Eur. Polym. J.*, 2007, **43**, 1857–1865.
41 M. Jorge, *Langmuir*, 2008, **24**, 5714–5725.
42 M. F. Lensink, C. Lonez, J.-M. Ruysschaert and M. Vandenbranden, *Langmuir*, 2009, **25**, 5230–5238.
43 C.-S. Ha and J. A. Gardella, *Chem. Rev.*, 2005, **105**, 4205–4232.
44 C. Shen, S. Guo and C. Lu, *Polym. Adv. Technol.*, 2008, **19**, 66–72.
45 C. Shen, S. Guo and C. Lu, *Polym. Degrad. Stab.*, 2007, **92**, 1891–1898.
46 G. S. Kwon, M. Yokoyama, T. Okano, Y. Sakurai and K. Kataoka, *Pharm. Res.*, 1993, **10**, 970–974.
47 C. Allen, N. D. Santos, R. Gallagher, G. N. C. Chiu, Y. Shu, W. M. Li, S. A. Johnstone, A. S. Janoff, L. D. Mayer, M. S. Webb and M. B. Bally, *Biosci. Rep.*, 2002, **22**, 225–250.
48 J. G. Wenzel, K. S. Balaji, K. Koushik, C. Navarre, S. H. Duran, C. H. Rahe and U. B. Kompella, *J. Controlled Release*, 2002, **85**, 51–59.
49 K. Ng and A. Rosenberg, *Thermochim. Acta*, 1990, **169**, 339–346.
50 R. Kjellander and E. Florin, *J. Chem. Soc., Faraday Trans. 1*, 1981, **77**, 2053–2077.
51 S. Lusse and K. Arnold, *Macromolecules*, 1996, **29**, 4251–4527.
52 O. Tirosh, Y. Barenholz, J. Katzhendler and A. Priev, *Biophys. J.*, 1998, **74**, 1371–1379.
53 C. Branca, S. Magaz, G. Maisano, F. Migliardo, P. Migliardo and G. Romeo, *J. Phys. Chem. B*, 2002, **106**, 10272–10276.
54 Y. K. Choi, Y. H. Bae and S. W. Kim, *Macromolecules*, 1998, **31**, 8766–8774.
55 P. J. Flory, *Principles of Polymer Chemistry*, Cornell University Press, Ithaca, NY, 1953, ch. 7.
56 P. Debye, *J. Chem. Phys.*, 1946, **14**, 636.

57 J. L. Koenig and A. C. Angood, *J. Polym. Sci., Part A-2*, 1970, **8**, 1787–1796.
58 S. Kuga, *J. Chromatogr., A*, 1981, **206**, 449–461.
59 K. Devanand and J. C. Selser, *Macromolecules*, 1991, **24**, 5943–5947.
60 H. Kuramochi, Y. Andoh, N. Yoshii and S. Okazaki, *J. Phys. Chem. B*, 2009, **113**, 15181–15188.
61 H. Lee, A. H. d. Vries, S.-J. Marrink and R. W. Pastor, *J. Phys. Chem. B*, 2009, **113**, 13186–13194.
62 S. J. Marrink, A. H. d. Vries and A. E. Mark, *J. Phys. Chem. B*, 2004, **108**, 750–760.
63 H. Lee, R. M. Venable, A. D. Mackerell, Jr and R. W. Pastor, *Biophys. J.*, 2008, **95**, 1590–1599.
64 C. M. Wijmans and E. B. Zhulina, *Macromolecules*, 1993, **26**, 7214–7224.
65 M. Daoud and J. P. Cotton, *J. Phys.*, 1982, **43**, 531–538.
66 H. Hyun, J. S. Cho, B. S. Kim, J. W. Lee, M. S. Kim, G. Khang, K. Park and H. B. Lee, *J. Polym. Sci., Part A: Polym. Chem.*, 2008, **46**, 2084–2096.
67 J. H. Lee, H. B. Lee and J. D. Andrade, *Prog. Polym. Sci.*, 1995, **20**, 1043–1079.
68 D. L. Elbert and J. A. Hubbell, *Annu. Rev. Mater. Sci.*, 1996, **26**, 365–394.
69 D. Needham, K. Hristova, T. J. McIntosh, M. Dewhirst, N. Wu and D. D. Lasic, *J. Liposome Res.*, 1992, **2**, 411–430.
70 D. Needham, T. J. McIntosh and D. D. Lasic, *Biochim. Biophys. Acta, Biomembr.*, 1992, **1108**, 40–48.
71 V. Toncheva, E. Schacht, S. Y. Ng, J. Barr and J. Heller, *J. Drug Targeting*, 2003, **11**, 345–353.
72 S. I. Jeon and J. D. Andrade, *J. Colloid Interface Sci.*, 1991, **142**, 159–166.
73 A. Halperin, *Langmuir*, 1999, **15**, 2525–2533.